Astron. Astrophys. 357, 725–734 (2000)

ASTRONOMY AND ASTROPHYSICS

Soft X-ray flares and magnetic configuration in a solar active region in February 1992

H.Q. Zhang[1], **T. Sakurai**[2], **K. Shibata**[2], **M. Shimojo**[2], **and H. Kurokawa**[3]

[1] Beijing Astronomical Observatory, National Astronomical Observatories, Chinese Academy of Sciences, Beijing 100012, P.R. China
[2] National Astronomical Observatory, Mitaka, Tokyo 181, Japan
[3] Kwasan and Hida Observatories, Kyoto University, Kyoto 606, Japan

Received 4 August 1999 / Accepted 13 December 1999

Abstract. In this paper, we examine the observational soft X-ray flares and the relationship with photospheric vector magnetograms in the active region (NOAA 7070). We analyze the soft X-ray flare on Feb. 24-25, 1992, especially the pre-flare and the relationship with the highly sheared photospheric vector magnetic field near the photospheric magnetic neutral line.

We find that the initial reconnection of the magnetic field in the flare on Feb. 24-25, 1992 probably occurs near the magnetic neutral line in the lower atmosphere of the active region, where the highly sheared magnetic flux erupts up and triggers the reconnection of the large-scale magnetic field. The possible process of the magnetic reconnection of the limb flare on Feb. 20-21, 1992 in this active region is proposed also based on the analogy with the flare on Feb. 24-25 near the center of the solar disk.

Key words: sun: activity – sun: flare – sun: magnetic fields

1. Introduction

The study of solar flares and the relationship with the magnetic field in solar active regions is an important topic in the solar physics. Since the launch of $Yohkoh$, a series of soft X-ray images of solar flares have been obtained by the Soft X-ray Telescope (SXT) (Tsuneta et al., 1991) on board the $Yohkoh$ satellite. It supplies important information on solar flares in the corona and reveals that compact loop brightening frequently occurs in some active regions. One of the important discoveries by the SXT is that of cusp-shaped loop structures in long duration event (LDE) flares (Tsuneta et al., 1992). The observed loop configuration of LDE flares and the relationship with the classical two-ribbons flare model (Carmichael, 1964; Strurrock, 1966; Hirayama, 1974; Kopp and Pneuman, 1997) were discussed by Shibata et al. (1995). It is important to study the photospheric magnetic field with the morphology of soft X-ray loop features for constructing the possible spatial configuration of the magnetic field above the photosphere. Information on the development of magnetic shear in solar active regions can be provided by photospheric vector magnetograms and chromospheric longitudinal magnetograms (Zhang, 1996). It is normally believed that solar flares are caused by the reconnection of the magnetic field in the corona, where the measurement of the magnetic field is very difficult. Thus extrapolation of the magnetic field from chromospheric and photospheric magnetograms and its relationship with the coronal morphological study become necessary for understanding the spatial configuration of the magnetic field in the solar active regions (such as, Sakurai, 1981; Sakurai et al., 1992; Mikic and McClymont, 1994; Amari, et al., 1996; Roumeliots, 1996; Yan and Sakurai, 1997). The questions are: what is the extension of the magnetic lines of force from the lower solar atmosphere to the corona and how does the interaction between the different magnetic lines of force trigger solar flares. It is an interesting problem and will be studied in this paper.

An active region (NOAA 7070) was observed with the $Yohkoh$ SXT and Vector Video Magnetographs at Huairou Solar Observing Station of Beijing Astronomical Observatory and National Astronomical Observatory of Japan, and also Domeless Solar Telescope at Hida Observatory of Kyoto University in February, 1992. During the passage of this active region across the solar disk, a series of flares occurred. This gave us a good chance to analyse the possible spatial configuration of these flares at the different positions (top or side) of view and the relationship with the magnetic field, especially the reconnection of the magnetic field during the flares, by the analytical combination between vector photospheric magnetograms and morphological configuration of flaring features in the chromosphere and corona.

In Sect. 2, we examine the soft X-ray flare on February 24-25, 1992, and also the relationship with the development of magnetic shear and electric current in the active region in the photosphere. In Sects. 3 and 4, we discuss the possible spatial configuration of the magnetic field above the active region, inferred by photospheric vector magnetograms, and the relationship with soft X-ray flares on February 20-21 and 24-25, 1992.

Send offprint requests to: H.Q. Zhang
Correspondence to: zhq@sun10.bao.ac.cn

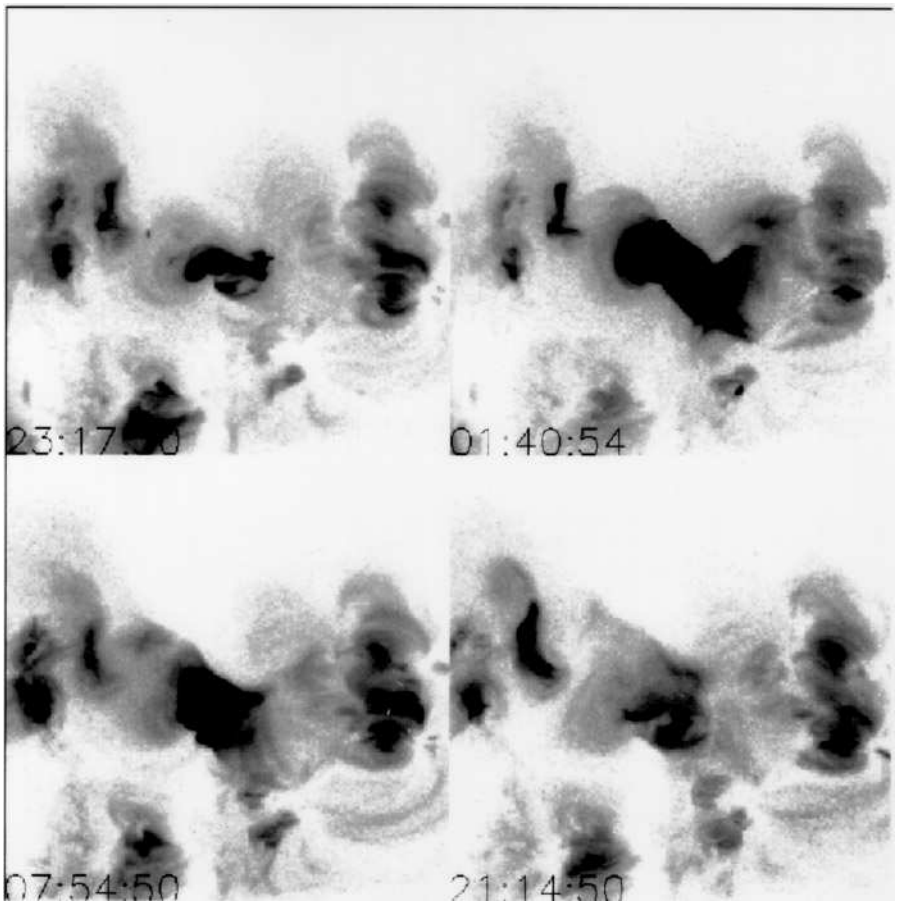

Fig. 1. A time sequence of soft X-ray images of the M4.9/2B flare on February 24–25, 1992. The size of images is $13' \times 13'$.

2. Soft X-ray flare on February 24-25, 1992

2.1. The M4.9/2B flare on February 24-25, 1992

Fig. 1 shows a series of soft X-ray images of the M4.9/2B flare on February 24-25, 1992 in the active region near the center of the solar disk. We can see that the soft X-ray loops quickly spread all over the space at the high solar atmosphere in the active region after the pre-flare stage. It provides the distribution of the soft X-ray flare loops in the top of view.

Fig. 2 shows the variation of bright loop features in the pre-flare stage. We can find the significant change of the X-ray feature occurred in the left side of the soft X-ray loop feature. This probably provides the information on the reconnection of the magnetic field in the pre-flare phase.

As one overlaps a soft X-ray image on the longitudinal magnetogram on February 25, 1992 in Fig. 3, we can find that the bright loop-like structure during the pre-flare phase in soft X-ray images connected the magnetic pole N_1 of positive polarity with the enhanced network magnetic field of negative polarity. Although the overlay between the soft X-ray image and magnetogram is adjusted by the photospheric image in the Yohkoh satellite, the soft X-ray image actually reflects the information of the hotter plasma, or rather, does not reflect the footpoints rooted in the cooler photosphere. This provides a basic relationship between the soft X-ray features and the photospheric magnetic field during the pre-flare phase in the active region (NOAA 7070).

2.2. Flare and non-potential magnetic field

Fig. 4 shows vector magnetograms near the center of the active region on February 24 and 25, 1992. The magnetic pole S_1 of negative polarity was located in the north relative to the positive polarity pole N_1. The transverse magnetic field is almost parallel to the magnetic neutral line between the poles N_1 and S_1. This means that the magnetic shear formed near the magnetic neutral line (cf. Hagyard et al., 1984). The negative magnetic pole S_2 was located away from pole N_2, and the transverse component of the photospheric magnetic field almost connected both poles (N_2 and S_2) on February 24. The separate speed between N_2 and S_2 is about 0.2 km/s. By comparing both vector magnetograms on Feb. 24 and 25 in Fig. 4, it is found that an amount of newly emerging magnetic flux occurs near the magnetic neutral line between magnetic poles N_2 and S_2, and these emerging magnetic features of opposite polarity tend to mix together to form some magnetic islands. These can be confirmed by the proper motion of features in the photospheric images (Kalman, 1997) and also the Hα and off-band filtergrams. The evidence of emerging magnetic flux can also be outlined by the soft X-ray movie that a series of small-scale bright features occurs near such an area on Feb. 21-25, 1992. These soft X-ray features

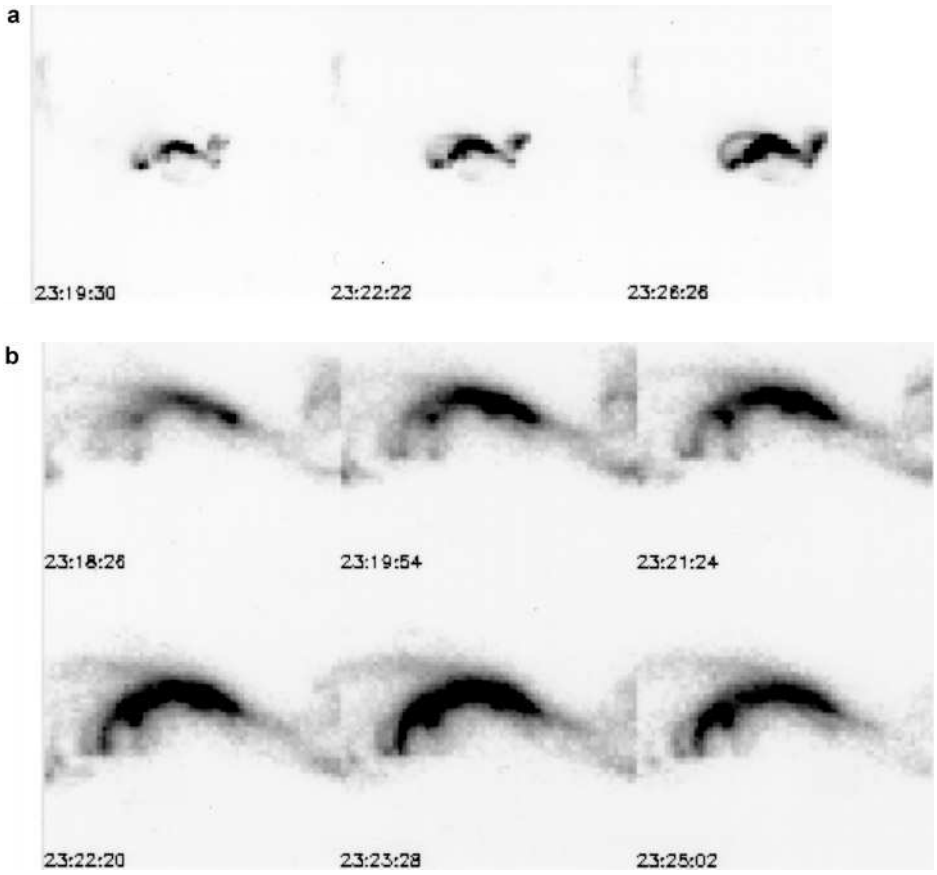

Fig. 2. a The variation of the soft X-ray images in the pre-flare stage on Feb. 24, 1992. The obvious change occurs near the left foot point of the large-scale soft X-ray loop. **b** The soft X-ray features in the pre-flare stage, which are the same with **a**, but the images are amplified by three times and the exposure is different. The change of the small-scale bright loop-like feature can be found in the left of the soft X-ray loop.

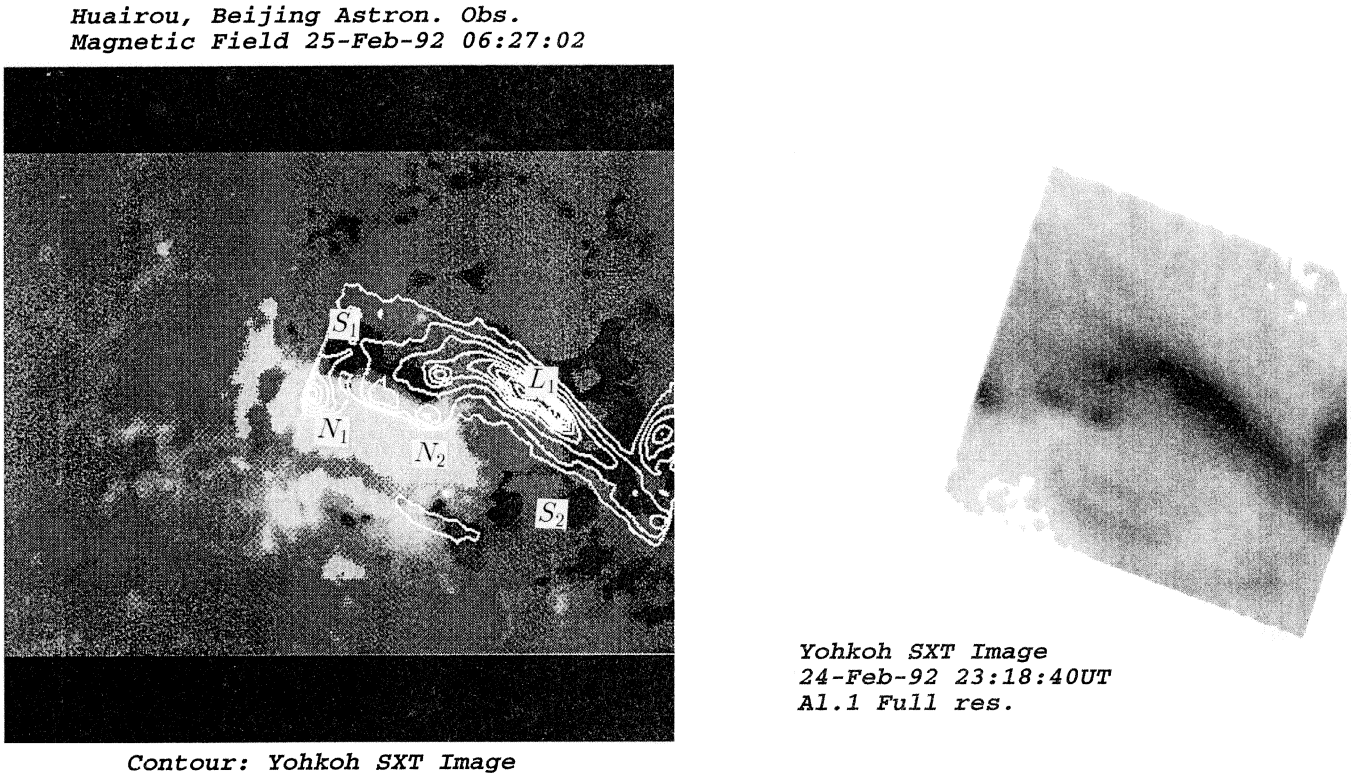

Fig. 3. A longitudinal magnetogram (left), overlaid by the soft X-ray image (right) by contour lines on February 25, 1992. The size of magnetogram is $4.'5 \times 3.'4$.

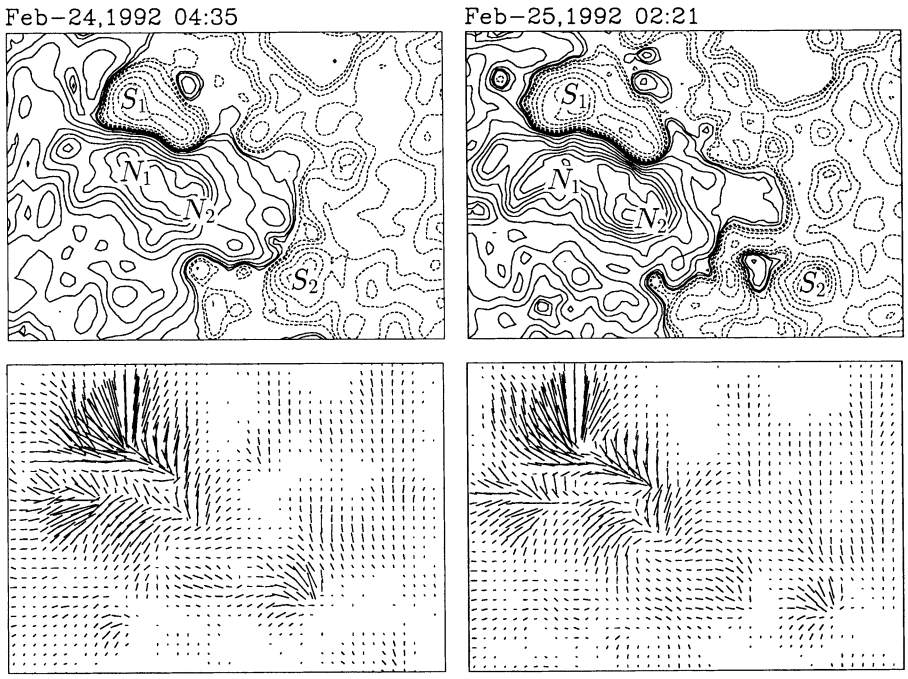

Fig. 4. Local vector magnetograms on February 24 (left) and 25 (right), 1992. The contour indicates the longitudinal magnetic field distribution, ±20, 160, 640, 1280, 1920, 2240, 2560, 2880 Gauss. The size of magnetograms is $2.'6 \times 1.'8$.

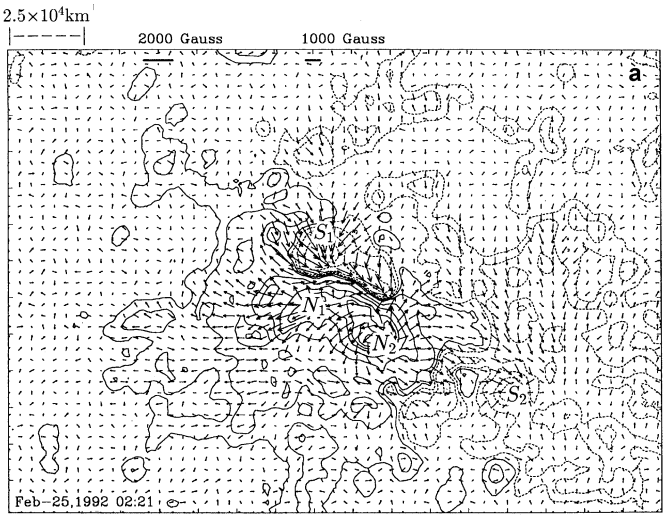

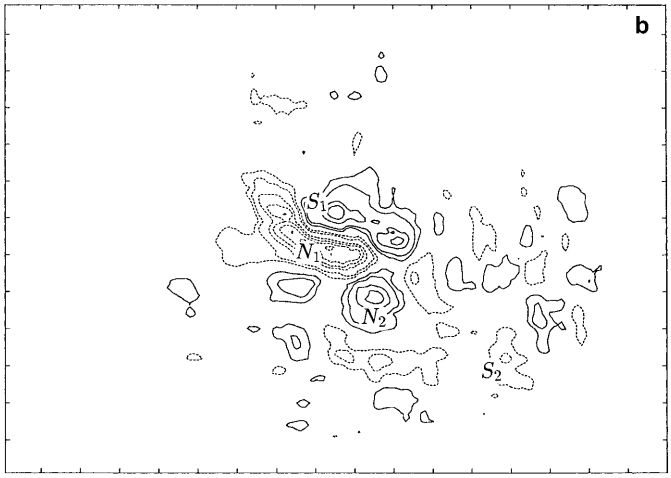

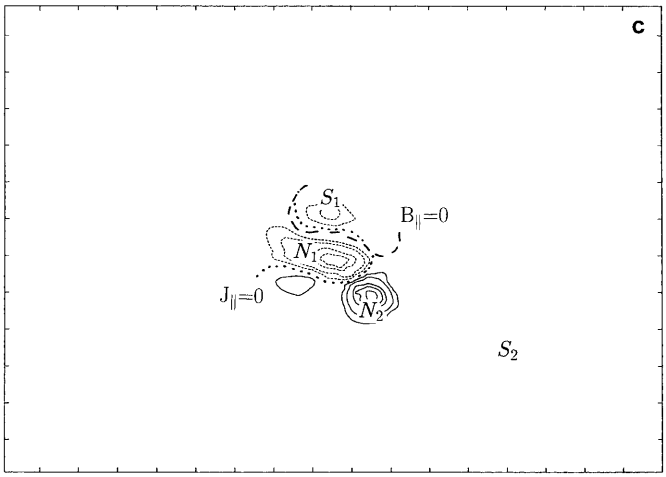

Fig. 5. a A vector magnetogram with the 180°-ambiguity of the transverse magnetic field resolved in the image plane in the active region (NOAA 7070) on February 25, 1992. The contour indicates the longitudinal magnetic field distribution, ±20, 160, 640, 1280, 1920, 2240, 2560, 2880 Gauss. **b** The corresponding longitudinal electric current (contour), ±0.2, 0.4, 0.8, 1.0, 1.4, 1.6, 2.0 ($\times 10^{-2}$)A m^{-2}. **c** The current helicity parameter $\mathbf{B}_{\|} \cdot (\bigtriangledown \times \mathbf{B})_{\|}$. The thick dashed line and dotted line mark the magnetic neutral line and the electric current inversion line respectively. The north is top and the east is at left.

probably are caused by that the new magnetic flux moves up and pushes the pre-existed magnetic field in the active region.

Fig. 5a shows a vector magnetogram on February 25, 1992. The 180°-ambiguity of the transverse component of the magnetic field is normally resolved by the approach of the potential field. The continuity of the direction of the transverse magnetic field is used in the vicinity of the highly sheared magnetic neutral lines, which does not influence the determination of the large-scale vertical electric current of the active region, even though this approach sometimes has given rise to some controversy.

Fig. 5b shows a map of the corresponding vertical electric current in the active region on February 25, 1992, which was inferred by the vector magnetogram. The calculation method of the vertical electric current by the Huairou vector magnetograms was discussed by Wang et al. (1994). Due to the noise level of about 100 Gauss for transverse field, the calculated vertical current has been spatially smoothed. This data deduction does not influence the basic estimation on the large-scale vertical electric current in the active regions, while the information on the small-scale current is lost. We can see that the distribution of the large-scale electric current in the active region is complex. The magnetic polarities do not have a unique relationship with directions of the vertical electric current. If the approximation of the force free field is roughly correct in the solar atmosphere, the flowing paths of the electric current can be inferred by following the track of magnetic lines of force and also the continuity of the transverse magnetic field in the photosphere. There are two current systems in this active region. A main electric current basically flows out from the magnetic pole S_1 of negative polarity and returns to the magnetic pole N_1 of opposite polarity at the high atmosphere. Another current system has oppositely directed current, i.e. the electric current probably flows out from the magnetic pole N_2 of positive polarity and returns to the magnetic pole S_2 of negative polarity.

The electric current helicity reflects the twist or linkage of the magnetic field. The density of current helicity can be written in the form

$$h_c = \mathbf{B} \cdot \bigtriangledown \times \mathbf{B} = \mathbf{B}_\perp \cdot (\bigtriangledown \times \mathbf{B})_\perp + \mathbf{B}_\parallel \cdot (\bigtriangledown \times \mathbf{B})_\parallel. \quad (1)$$

In the approximation of the force free field,

$$h_c = \alpha B^2 = (B/B_\parallel)^2 \mathbf{B}_\parallel \cdot (\bigtriangledown \times \mathbf{B})_\parallel, \quad (2)$$

where α is not constant. The second term (i.e. $\mathbf{B}_\parallel \cdot (\bigtriangledown \times \mathbf{B})_\parallel$) of the current helicity density in Eq. (1) can be obtained by the photospheric vector magnetogram. As we normally believe that in the strong magnetic poles the magnetic field is almost vertical to the solar surface, then the current helicity density parameter $\mathbf{B}_\parallel \cdot (\bigtriangledown \times \mathbf{B})_\parallel$ near the center of the magnetic poles probably reflects the basic handedness of the twisted poles, while the current helicity density parameter $\mathbf{B}_\perp \cdot (\bigtriangledown \times \mathbf{B})_\perp$ mainly provides the information near the magnetic neutral line etc., where the transverse field $\mathbf{B}_\perp$ is dominant. So the current helicity density parameter $\mathbf{B}_\parallel \cdot (\bigtriangledown \times \mathbf{B})_\parallel$ reflects the basic information on the twist of the magnetic poles in the active region (Zhang and Bao, 1998). (The current helicity density parameter $\mathbf{B}_\perp \cdot (\bigtriangledown \times \mathbf{B})_\perp$

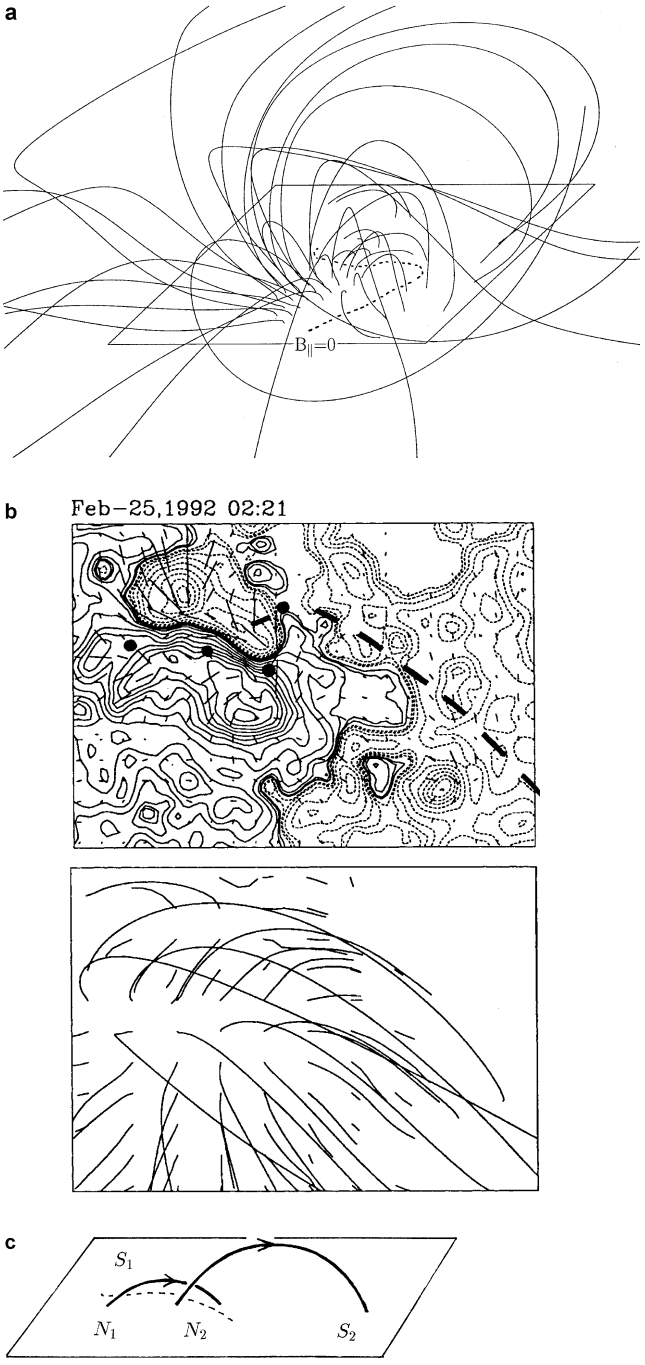

Fig. 6. The magnetic lines of force extrapolated by using a constant-α force free field model in the active region (NOAA 7070) on February 25, 1992. **a** Distribution of the magnetic lines of force in the whole of active region in the side view. The dotted line indicates the magnetic neutral line. **b** The vector magnetogram (top diagram) and the distribution of magnetic lines of force above the photosphere in the center of active region in the top view (bottom diagram). Black large circles mark the positions of the soft X-ray bright points in both sides of the highly sheared magnetic neutral line, and the thick dashed line marks the position of the soft X-ray loop L_1 in the pre-flare stage. **c** A possible scheme of the spatial configuration of the magnetic field above the photosphere in the active region. The thick arrow lines mark the magnetic lines of force along L_1 (right) and highly sheared ones (left) near magnetic neutral line.

has been very difficult to obtain by the photospheric vector magnetograms until now.) From a map of the current helicity density parameter $\mathbf{B}_{\|} \cdot (\bigtriangledown \times \mathbf{B})_{\|}$ in Fig. 5c, we can easily find that the local current helicity in the photosphere of the active region can be obviously separated into two parts, if we follow the discussion above and the continuity of the photospheric transverse field. One shows negative sign and connects with the sheared magnetic field region (N_1 and S_1), and another shows positive sign and is located near the magnetic pole N_2. If we follow the direction of the photospheric transverse magnetic field and the sign of the electric current, the region with the positive helicity also contains the magnetic pole S_2 and probably the surrounding enhanced magnetic network near the magnetic pole S_2. This means that two parts with opposite signs of the electric current helicity in the active region show oppositely twisted characteristics of the magnetic field.

3. Spatial configuration of the magnetic field

By comparing the vector magnetogram with the corresponding soft X-ray image overlapping on the longitudinal magnetogram (Figs. 3 and 4), we can find that the bright loop-like structure L_1 on February 25, 1992 in soft X-ray images connected magnetic pole N_1 of positive polarity with the enhanced network magnetic field of negative polarity. It is found that the soft X-ray feature L_1 is not always running along the direction of the transverse component of the photospheric magnetic field, although the soft X-ray loop probably reflects the information of the magnetic field in the corona. In the east end of the soft X-ray loop, the relationship with the photospheric transverse magnetic field is relatively complex. The similar pattern of bright soft X-ray features between the magnetic poles N_2 and S_2 of opposite polarity was discussed by Kurokawa et al. (1994).

Because the measurement of the coronal magnetic field is difficult, the extrapolation of the photospheric magnetic field to the high atmosphere becomes very important for the analysis of the spatial configuration of the magnetic field. The complex sign distribution of photospheric current helicity density in the active region NOAA 7070 means that this active region is a departure from the approximation of the constant α force free field. Even though, we also can use the force free field with a constant α to fit the spatial configuration of the magnetic field in the active region, as this α can be used to match the large-scale field above the photosphere. Fig. 6a shows the distribution of magnetic lines of force above the photosphere, which is calculated by the approximation of the constant-α force free magnetic field (Chiu and Hilton, 1977), where α is 0.3 (the unit is $10^{-4}\mathrm{km}^{-1}$), and the photospheric boundary in the extrapolated calculation is the longitudinal magnetic field in Fig. 5a. It provides a rough distribution of magnetic lines of force above the solar photosphere. In Fig. 6b, the thick dashed line shows the position of the pre-flare soft X-ray loop L_1. We can see that L_1 is almost parallel to the calculated magnetic lines of force. This probably provides the information that the coronal mass was heated along the magnetic lines of force near the interface between different magnetic field (electric current) systems, due to their interaction in the pre-flare stage. Moreover, it is notice that the highly sheared transverse magnetic field occurs near the magnetic neutral line between magnetic poles (N_1 and S_1) of opposite polarity, and it is obviously a departure from the extrapolated field lines due to the approximation of the constant α force free field. For analyzing the morphological configuration of the magnetic field, Fig. 6c shows an ideal scheme of the possible configuration of the magnetic lines of force near magnetic neutral line in the active region, which is inferred by the photospheric vector magnetogram and its relationship with the soft X-ray features in Figs. 2, 3 and 4b. An mount of non-potential magnetic energy probably stores near the highly sheared magnetic neutral line above the photosphere in the active region.

In this paper, we do not discuss such sudden changes of the photospheric vector magnetic field during the flare, because we did not get such a series of vector magnetograms before and after the flares. However, we find that the change of shear angles of the transverse magnetic field between magnetic main poles (N_1 and S_1) is insignificant on Feb. 24-25, 1992, even if we can not infer that the photospheric magnetic shear is kept by the emergence of new magnetic flux, while the obvious structural evolution of the magnetic field in the vicinity between magnetic main poles (N_2 and S_2) on February 24-25, 1992 can be found in Fig. 4. By following the morphology of the initial flares and the relationship with the photospheric vector magnetic field in Figs. 2, 3 and 4, the possible mechanism of the flares can be inferred. We can find that a small-scale bright soft X-ray loop-like feature occurred in the east end of the soft X-ray loop L_1 and bridged over the magnetic neutral line between the magnetic main poles N_1 and S_1 of opposite polarities. This probably implies that the interaction of the magnetic field occurs near the magnetic neutral line at the lower solar atmosphere in Fig. 6c. The interaction between the magnetic lines of force and the highly sheared magnetic field causes the reconnection of the magnetic field, then forms newly connected magnetic lines of force. A part of them erupts up and pushes into the large-scale overlying magnetic field, that connects the photospheric magnetic main poles of opposite polarities, to trigger the reconnection of the large-scale magnetic field (M4.9/2B flare on February 24-25) above the photosphere in the active region. This means that the magnetic energy stored near the highly sheared magnetic neutral line are enough to trigger the powerful flares (Moore, et al., 1995; Amari, et al., 1996,1999).

4. Comparing with soft X-ray flare on February 20-21, 1992

Another soft X-ray flare on February 20-21, 1992 in this active region was analyzed by several authors (such as Tsuneta, et al., 1992; Hudson, 1994). It provides the information on the configuration of the soft X-ray flare in the side of view. For analyzing the possible spatial configuration of flares and the relationship with the magnetic field, we first study the distribution of the magnetic field in the active region near the solar limb and its possible evolution.

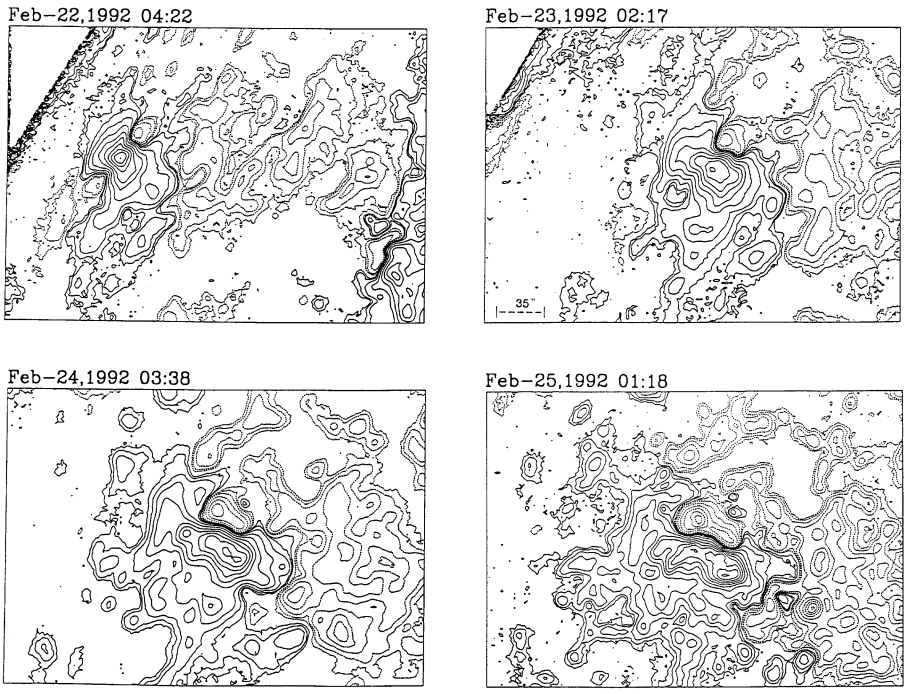

Fig. 7. A series of longitudinal magnetograms in active region 7070 in February 1992. The contour indicates the longitudinal magnetic field distribution, ±20, 160, 640, 1280, 1920, 2240, 2560, 2880 Gauss. The north is top and the east is at left. The size of magnetograms is $5.'2 \times 3.'6$.

4.1. Evolution of the magnetic field in the active region

Fig. 7 shows a series of longitudinal magnetograms in the active region 7070 on February 22-25, 1992. In spite of the evolution of magnetic features and the size change of the active region due to the projection effect of the magnetic field as the solar rotation, we can find that the basic configuration of the magnetic field in this period is almost the same. The large-scale magnetic field in the active region shows a typical bipolar distribution of the magnetic polarity.

On the other hand, the resolution of 180°-ambiguity of the transverse component of the magnetic field near the highly sheared magnetic neutral line is a notable problem, and must be carefully examined in the complex magnetic configuration. We need to point out that this ambiguity near the magnetic neutral line does not influence the basic analysis of the twist of the magnetic poles in the active region. Actually, the ambiguity of the magnetic field has been roughly resolved by the continuity of the field near magnetic neutral line, such as that between magnetic poles (N_1 and S_1) in the active region.

4.2. Soft X-ray flare on February 20-21, 1992 near the solar limb

It is often observed that a flare brightens in exactly the same position and exhibits the same geometrical outline as the previous flare in that region. These flares are named the homologous flares (Tandberg-Hanssen and Emslie, 1988). It is commonly believed that homologous flares are triggered by the same mechanism. We probably can infer the real spatial configuration of soft X-ray flares by observing homologous flares over time, since the homologous flares from the same active region occur in the different positions of the solar disk due to the solar rotation.

A series of flares occurred in the active region of February 1992. The similarity of these flares was discussed by Morita et al. (1998). Now, we study the soft X-ray flare on Feb. 20-21, 1992. We can see a small "helmet streamer"-like structure near the solar surface, with a loop-like feature overlaid on it at 23:52:42 UT on Feb, 20, 1992 in Fig. 8. The similar configuration is not easily seen in the image obtained at 20:40:44 UT on Feb. 24, 1992, due to the background emission of the solar disk and the perspective effect of the soft X-ray features. As we follow the evolution of the soft X-ray features in the movie, we can find that the initial bright soft X-ray features during the pre-flare phase almost occurred at the same position in the active region (NOAA 7070).

The reconnected magnetic fields above the photosphere in the post flare stage generally can be approximated by a potential magnetic field (Svestka, et al., 1987). We can extrapolate the potential field from the photospheric longitudinal magnetogram of Feb. 25, 1992. As this magnetogram is rotated to the position at the time of the flare on Feb. 21, 1992 in Fig. 9, we find that the distribution of the large-scale photospheric longitudinal magnetic field on Feb. 25 is almost the same to that on Feb. 21. Their difference probably is caused by the projection effect and evolution of the photospheric magnetic field. The extrapolated magnetic field lines in the high atmosphere almost coincides with that of the post flare soft X-ray loops of Feb. 21, 1992. By excluding some magnetic lines of force in the northern side of the active region (these magnetic lines of force do not show the corresponding bright soft X-ray features), we find that the magnetic lines of force show almost the same tendency of the inclination of the magnetic field loops with the height. Both foot points of the flare loops are located in the large-scale photospheric magnetic poles of opposite polarity. This also means

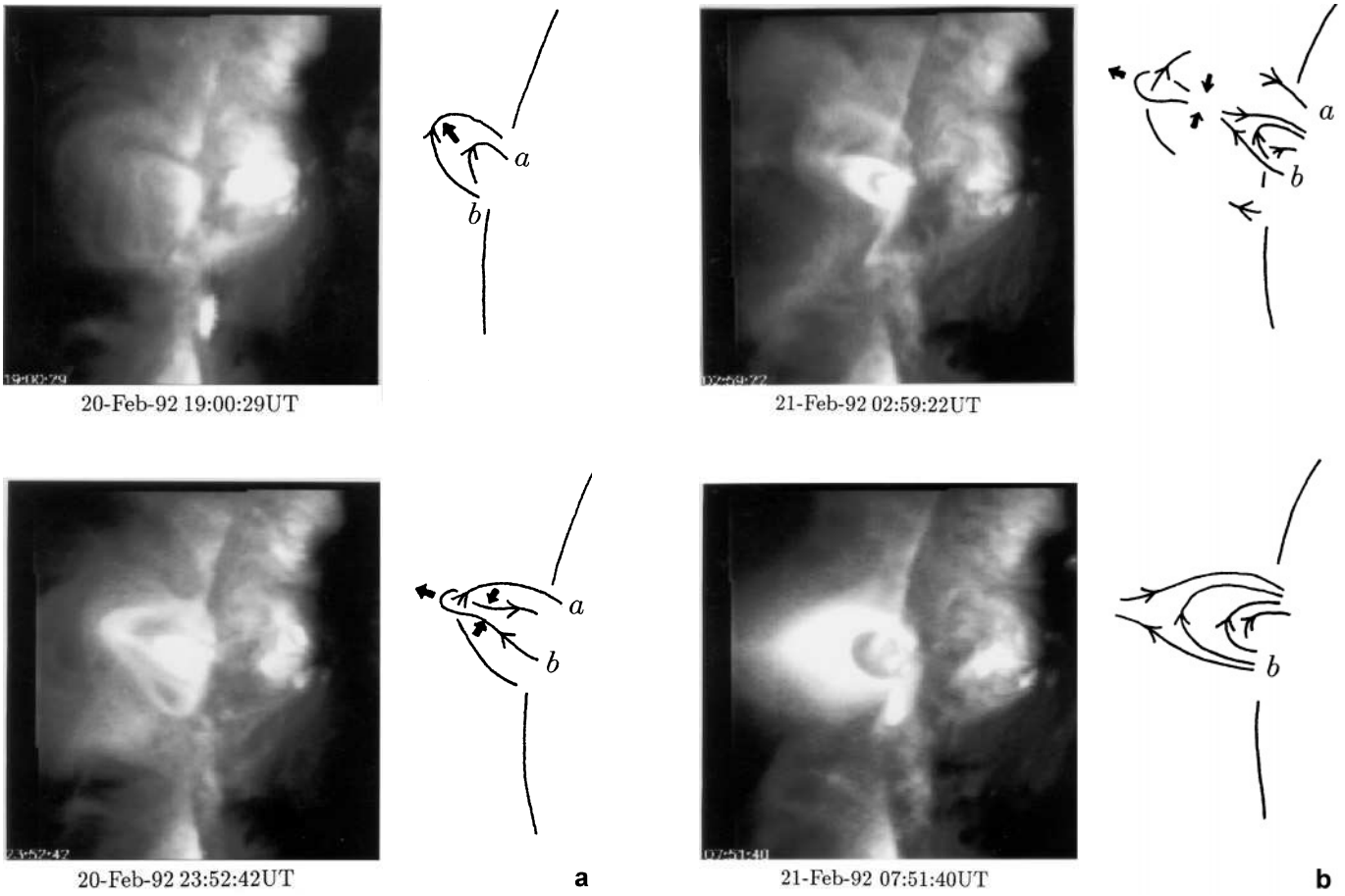

Fig. 8. A time sequence of the soft X-ray flare on 20–21 Feb. 1992 (left). The reconnection process of the magnetic lines of force in the period of the soft X-ray flare is inferred by homologous flares in the active region in February 1992 (right). The arrow lines show the magnetic lines of force above the photosphere in the active region. The short arrows indicate the moving direction of magnetic lines of force. a and b mark the topological correspondence of magnetic lines of force.

that the change of the basic topology of the magnetic field is not significant, and thus the spatial configuration of the soft X-ray flare on Feb. 21, 1992 can be roughly inferred by that of the flare homologous to it on Feb. 25, 1992. Similar evidence can also be found by the series of daily magnetograms in Fig. 7, e.g. the distribution of the large-scale magnetic field is almost similar, if the perspective effect of the magnetic field is considered.

Fig. 8 shows a time sequence of soft X-ray images on Feb. 20-21, 1992. If these features in the soft X-ray images reflect the distribution of the coronal magnetic field in the solar active region, we can infer a possible process of magnetic reconnection during the soft X-ray flares in the active region. The magnetic field reconnection hypothesis is: (a) The initial reconnection of the magnetic lines of force occurs near the magnetic neutral line due to the interaction between the highly sheared magnetic flux and pre-existing magnetic field of opposite polarity, where the instability of the magnetic field occurs. (b) The reconnected magnetic lines of force move up and push into the overlying magnetic field connected with the large-scale photospheric magnetic structures of opposite polarities in the active region. (c) Reconnection of the large-scale magnetic field occurs under the erupting magnetic lines of force and a cusp-shaped loop structure forms. (d) Closed magnetic rings are created high above the reconnection region of the magnetic lines of force and move away. (e) After the LDE flare, the non-potential magnetic energy is stored continuously in the active region and eventually triggers the next flare after the emergence of highly sheared magnetic flux near the magnetic neutral line.

5. Discussion and results

In active regions, the reconnection of the magnetic field to trigger the flare is a notable problem, because it concerns the fast transformation of amount of magnetic energy in the high solar atmosphere and can not be immediately measured by any magnetographs. In the active region (NOAA 7070), the sudden brightening of small-scale soft X-ray loop-like features above the photospheric magnetic neutral line before the powerful flares actually reflects the reconnection of the magnetic lines of force. In comparing the soft X-ray features with the photospheric vector magnetograms, we probably can construct the possible spatial configuration of the magnetic field and the reconnection of magnetic field in the active region. In the active

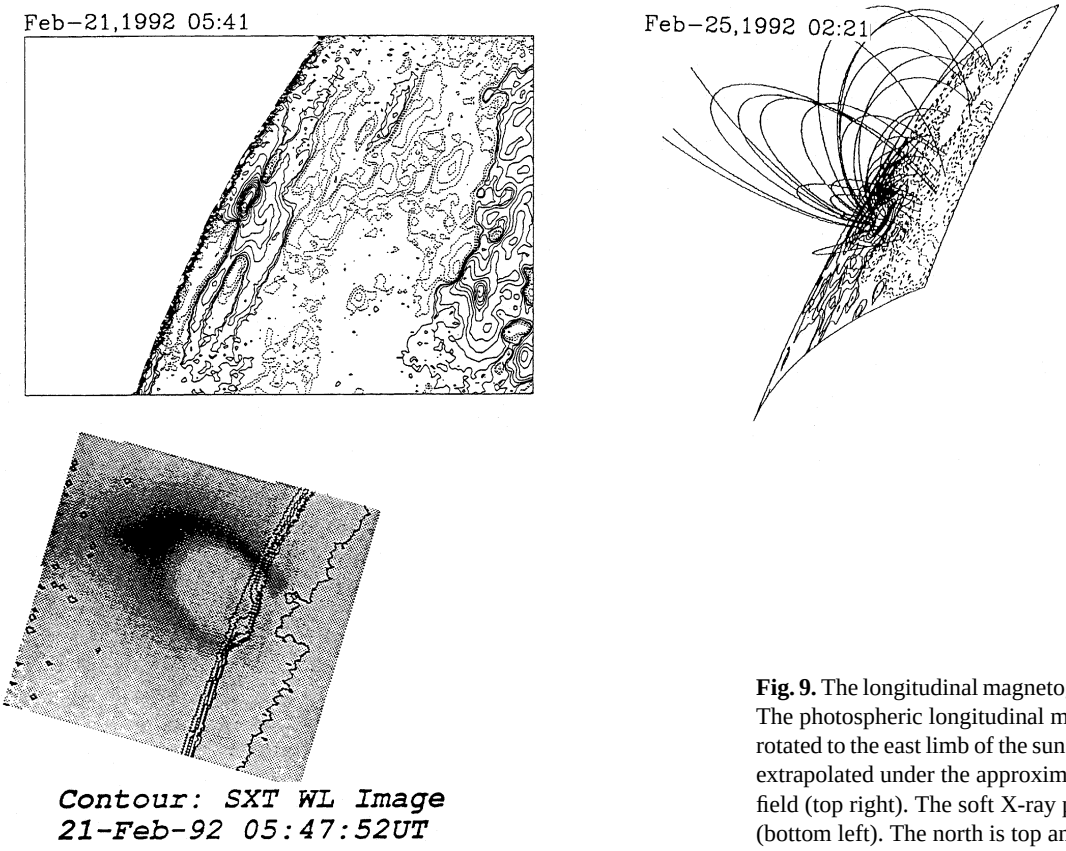

Fig. 9. The longitudinal magnetogram on 21 Feb. 1992 (top left). The photospheric longitudinal magnetogram of 25 Feb. 1992 is rotated to the east limb of the sun and the magnetic field lines are extrapolated under the approximation of the potential magnetic field (top right). The soft X-ray post flare loop on 21 Feb. 1992 (bottom left). The north is top and the east is at left.

region (NOAA 7070), the reconnection of the magnetic field firstly occurs near the magnetic neutral line above the photosphere, then the reconnected magnetic lines of force erupt up, and push the overlying large-scale magnetic field to become open or partly open magnetic field. Subsequent reconnection of the large-scale open magnetic field can be inferred by the soft X-ray flares and the foot points of the magnetic field in the chromosphere by Hα and Hβ flare ribbons. From the discussion above, we can understand that an amount of non-potential magnetic energy is probably stored near the highly sheared magnetic neutral line above the photosphere. The interaction between the highly sheared magnetic flux near the magnetic neutral line and the pre-existing magnetic field probably causes the instability of the field to trigger the reconnection of the large-scale magnetic field in the active region. The pre-flare sheared field normally contains enough non-potential magnetic energy of the order needed to fuel a great flare such as ours (Moore et al., 1995).

After the analysis, the main results are the following.

(1) The active region (NOAA 7070) is a flare-producing region. The configuration of the magnetic field is consistent with the presence of two main systems of magnetic lines of force. These two systems show opposite signs of the current helicity. Due to the interaction between the different systems of magnetic lines of force, the soft X-ray brightening occurs near the interface between the different systems.

(2) A series of flares in active region (NOAA 7070) was caused by the interaction between different magnetic lines of force. The brightening of small-scale soft X-ray loop-like features, which occurred near the magnetic neutral line, probably reflects the reconnection of the magnetic field in the pre-flare stage. The reconnection of the large-scale magnetic field in the active region probably is triggered by the pre-flare reconnection of the highly sheared magnetic field occurred near the magnetic neutral line at the lower atmosphere.

Acknowledgements. The authors would like to thank the $Yohkoh$ team for their observations. The author (HQZ) would like to thank Dr. T. Sakurai for the kind invitation to visit National Astronomical Observatory of Japan and also to thank Mrs. K. Kano and J. Shin for their assistances at the study of the $Yohkoh$ soft X-ray data. The authors would like to thank Dr. Y. Liu for the discussion of the force free magnetic field and Dr. T. J. Wang for the calculation of the electric current helicity. The authors also would like to thank the referee's comments and suggestions for the improvement of the manuscript. This study is also supported by Chinese Academy of Sciences and National Science Foundation of China.

References

Amari T., Luciani J.F., Aly J.J., Tagger M., 1996, A&A 306, 913
Amari T., Luciani J.F., Mikic Z., Linker J., 1999, ApJ 518, L57
Carmichael H., 1964, In: Hess W.H. (ed.) Proc. AAS-NASA Symp. on the Physics of Solar Flares. NASA, Washington, NASA-Sp 50, p. 451
Chiu Y.T., Hilton H.H., 1977, ApJ 212, 873
Hagyard M.J., Smith J.B., Teuber D., West E.A., 1984, Solar Phys. 91, 115

Hirayama T., 1974, Solar Phys. 34, 323
Hudson H.S., 1994, In: Enome S., Hirayama T. (eds.) Proc. of Kofu Symposium, NRO Report No. 360, p. 1
Kalman B., 1997, A&A 327, 779
Kopp R.A., Pneuman G.W., 1976, Solar Phys. 50, 85
Kurokawa H., Kawai G., Tsuneta S., Ogawara Y., 1994, In: Uchida Y., Watanabe T., Shibata K., Hudson H.S. (eds.) X-ray Solar Physics From Yohkoh. University Academy Press Inc., p. 59
Mikic Z., McClymont A.N., 1994, Solar Active Region Evolution. ASP Conf. 68, 225
Moore R.L., LaRosa T.N., Orwig L.E., 1995, ApJ 438, 985
Morita S., Uchida Y., Fujisaki K., Hirose S., 1998, In: Watanabe T., Kosugi T., Sterling A.C. (eds.) Proc. Yohkoh 5th Anniversary Symposium, p. 327
Roumeliotis G., 1996, ApJ 473, 1095
Sakurai T., 1981, Solar Phys. 69, 343
Sakurai T., Shibata K., Ichimoto K., Tsuneta S., Acton L.W., 1992, PASJ 44, L123
Shibata K., Masuda S., Shimojo M., et al., 1995, ApJ 451, L83
Strurrock P.A., 1966, Nat 211, 695
Svestka S., Fontenla J.A., Machado M.E., Martin S.F., Poletto G., 1987, Solar Phys. 108, 237
Tandberg-Hanssen E., Emslie A.G., 1988, The Physics of Solar Flares. Cambridge Uni. Press
Tsuneta S., Acton L., Bruner M., et al., 1991, Solar Phys. 136, 37
Tsuneta S., Takahashi T., Acton L., et al., 1992, PASJ 44, L63
Wang T.J., Xu A.A., Zhang H.Q., 1994, Solar Phys. 155, 99
Yan Y.H., Sakurai T., 1997, Solar Phys. 174, 65
Zhang H., 1996, ApJ 471, 1049
Zhang H., Bao S., 1998, A&A 339, 880